Oxygen-18 Kinetic Isotope Effects in the Dopamine β-Monooxygenase Reaction: Evidence for a New Chemical Mechanism in Non-Heme Metallomonooxygenases†

Gaochao Tian,‡,§ Joseph A. Berry,‖ and Judith P. Klinman*,‡

Department of Chemistry, University of California, Berkeley, California 94720, and Department of Plant Physiology, Carnegie Institute of Washington, 290 Panama Saint, Stanford, California 94305

Received July 9, 1993; Revised Manuscript Received October 8, 1993®

ABSTRACT: Previous studies of dopamine β-monooxygenase (DβM) have implicated the formation of a substrate-derived benzylic radical via a hydrogen atom abstraction mechanism [Miller & Klinman (1985) *Biochemistry 24*, 2114]. We now address the nature of the oxygen species catalyzing C–H bond cleavage through the measurement of oxygen-18 isotope effects as a function of substrate structure. Using deuterium isotope effects, together with experimental O-18 isotope effects with protonated and deuterated substrates, it has been possible to calculate intrinsic O-18 isotope effects. Since the DβM mechanism includes many steps which may involve changes in bond order at dioxygen, e.g., the reversible binding of O_2 to the active-site copper and its reductive activation to a copper–hydroperoxide species, the intrinsic O-18 isotope effect is expected to be the product of two terms: (1) an overall equilibrium O-18 isotope effect on steps leading from O_2 binding to the formation of the intermediate which catalyzes C–H bond cleavage and (2) a kinetic O-18 isotope effect on the C–H bond cleavage step. Thus, the magnitude of a single O-18 isotope effect measurement cannot reveal the nature of the bonding at oxygen during substrate activation. In the present study we have measured the change in O-18 isotope effect as a function of substrate structure and reactivity, finding values of $^{18}(V/K)$ which decrease from 1.0281 ± 0.001 to 1.0216 ± 0.0003 as the rate of the C–H bond cleavage step decreases from 680 to 2 s^{-1}. As described, this trend in O-18 isotope effect with reactivity can only be explained if the O–O bond of dioxygen undergoes cleavage prior to substrate activation. A new chemical mechanism is proposed for DβM which may serve as a general paradigm for non-heme, metallomonooxygenases.

Activation of ground-state, spin-unpaired dioxygen is a necessary process in a wide range of biological redox processes. In many enzymic systems, this is achieved through the interaction of dioxygen with metal ion cofactors. Consequently, elucidation of the activated metal–oxygen species is crucial to our understanding of the chemistry of the enzymatic oxidative transformations. Various spectroscopic methods, such as EPR,[1] Raman, UV–visible, and X-ray absorption techniques, have been used toward this end, leading to considerable insight into the structure of activated species. In many cases, however, activated metal–oxygen intermediates are very short-lived and hence extremely difficult to observe directly. Complementary to the use of spectroscopic methods, model studies can provide a great deal of insight into the nature of activated oxygen species. When model studies are inaccessible or the lifetime of activated species is too short to allow direct observation, description of reactive intermediates much rely on inferences derived from indirect evidence. In such instances, development of new methods becomes highly desirable. In a previous study, we have described the use of O-18 isotope effects to characterize the nature of the metal–oxygen species formed upon binding of dioxygen to the naturally occurring reversible oxygen carriers hemoglobin, myoglobin, hemerythrin, and hemocyanin (Tian & Klinman, 1993). In this paper, we report the application of O-18 isotope effects toward the elucidation of the mechanism of O_2 activation in a monooxygenase reaction, that of dopamine β-monooxygenase.

Dopamine β-monooxygenase (DβM) catalyzes the transformation of dopamine to norepinephrine, an important neurotransmitter in mammals. As illustrated

$$RCH_2CH_2NH_2 + O_2 \xrightarrow{2H^+,\,2e^-} RCHOHCH_2NH_2 + H_2O \quad (1)$$

one oxygen atom from dioxygen is inserted into the benzylic position of dopamine while the other oxygen atom is transformed to water. Two exogenous electrons are provided by ascorbate (Terland & Flatmark, 1975), which is generally assumed to be the *in vivo* reductant. Because of the biological importance of DβM, the enzyme has been subjected to extensive scrutiny. As reviewed (Stewart & Klinman, 1988), DβM exists as active dimeric and tetrameric species. With the exception of the degree of glycosylation and small differences at the N-terminus, the structure of each subunit is identical and contains two catalytically essential copper atoms. The ligands to copper are predominantly histidines; additionally, a single copper atom has been proposed to be coordinated to a sulfur atom in its reduced, Cu(I) form. Given the absence of three-dimensional structural information, further identification of active-site residues has relied on enzyme labeling by mechanism-based inhibitors. Detailed work of this nature has implicated several tyrosines at or near the enzyme active site, Tyr-216 and Tyr-357 (Fitzpatrick & Villafranca, 1987; DeWolf et al., 1988).

In an effort to gain insight into the role of the copper centers in DβM catalysis, rapid mixing experiments have been explored

† Supported by grants from the NIH (GM 25765 to J.P.K.), AHA (91-34 to G.T.), and U.S. DOE (FG0586 ER3563 to J.A.B.). This is CIW-DPB Publication 1161.

* To whom correspondence should be addressed.

‡ University of California, Berkeley.

§ Current address: Glaxo Inc., 5 Moore Dr., Research Triangle Park, NC 27709.

‖ Carnegie Institute of Washington.

® Abstract published in *Advance ACS Abstracts*, December 1, 1993.

[1] Abbreviations: EPR, electron paramagnetic resonance; DβM, dopamine β-monooxygenase; EXAFS, extended X-ray absorption fine structure.

0006-2960/94/0433-226$04.50/0

Scheme 1: Schematic Illustration of the Two Copper Sites per Subunit of DβM[a]

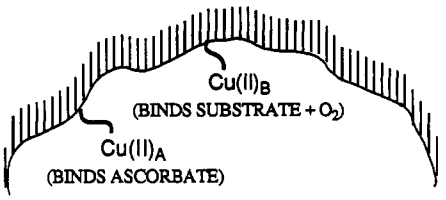

[a] This scheme shows the two copper sites performing separate functions of electron transport from ascorbate [$Cu(II)_A$] and substrate hydroxylation [$Cu(II)_B$].

to examine the reduction of enzyme-bound copper by ascorbate and reoxidation of copper by substrate and dioxygen (Brenner & Klinman, 1989). Both coppers in free enzyme were found to be reduced by ascorbate in a rapid, single-exponential process. Reoxidation of the reduced copper by substrate and O_2 also occurred in a single-exponential process, with a rate constant which is essentially identical to that for formation of enzyme-bound product. Importantly, no evidence for spin coupling has been detected in resting enzyme (Klinman & Brenner, 1988; McCracken et al., 1988) or in the catalytically generated product complex (Brenner & Klinman, 1989). These results, together with the failure of EXAFS experiments to detect back scattering between copper centers (Scott et al., 1988), argue that the two copper atoms are at least 4 Å apart in the E and E·P complexes and hence that catalysis is unlikely to involve a binuclear center of the type observed in tyrosinase and hemocyanin (Solomon et al., 1993). Unexpectedly, the E·P complex has been found to undergo reduction by high levels of ascorbate, indicating that product and ascorbate can bind to enzyme at the same time (Brenner & Klinman, 1989). On the basis of the available data, a model has been put forth in which the two copper centers in DβM perform separate functions, that of electron transfer, $Cu(II)_A$ site, and substrate hydroxylation, $Cu(II)_B$ site (Scheme 1). The findings of Blackburn et al. (1990), showing that carbon monoxide is competitive toward O_2 at a single copper site per subunit, provide experimental support for this view of catalysis.

A major challenge has been to describe the chemical steps leading from the complex of substrate and O_2 to hydroxylated product at a single copper center. Early studies of pH-dependent isotope effects indicated an absolute requirement for proton uptake prior to substrate hydroxylation, attributed to the formation of a copper hydroperoxide species functioning in C–H bond cleavage (Ahn & Klinman, 1983). Detailed structure function studies using either substrates (Miller & Klinman, 1985) or mechanism-based inhibitors (Fitzpatrick & Villafranca, 1985) have implicated a benzylic radical as a catalytic intermediate, and it is generally accepted that the DβM reaction occurs via a hydrogen atom abstraction mechanism. By contrast, little has been known regarding the oxygen species responsible for substrate activation, in particular whether this is copper hydroperoxide itself (eq 2) or a copper–oxo species derived from copper hydroperoxide (eq 3). The copper hydroperoxide mechanism (eq 2) has been favored in the past, on the basis of thermodynamic considerations: as described by Miller and Klinman (1985), a concerted mechanism in which the energy released upon hydrogen transfer from carbon to oxygen is coupled to O–O bond cleavage at Cu–OOH is feasible. Such a mechanism was shown to be compatible with a close to thermoneutral H transfer process and hence the large intrinsic deuterium isotope effect observed on the C-H cleavage step (Miller & Klinman, 1983). Although the copper hydroperoxide mechanism was

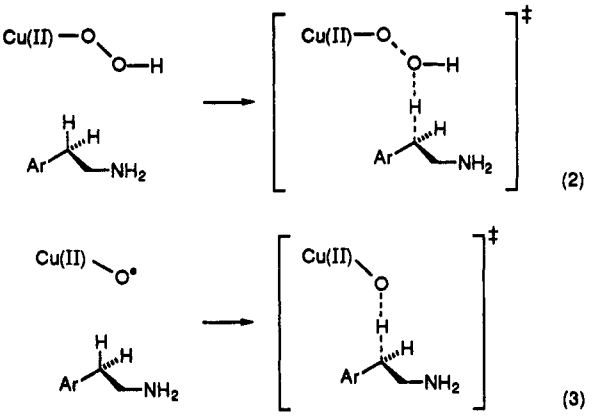

able to rationalize existing data, it has not been possible to rule out a requisite cleavage of the Cu–OOH bond prior to substrate activation (eq 3). We have now developed an experimental method to investigate the nature of the oxygen species catalyzing C–H bond cleavage. As described, this approach involves measuring perturbations in the magnitude of intrinsic O-18 isotope effects as a function of perturbations in substrate structure and inherent chemical reactivity. *Unexpectedly, these results lead to the conclusion that an active-site copper hydroperoxide must undergo reductive cleavage prior to substrate activation. A new mechanism is put forth for dopamine β-monooxygenase, which may serve as a general paradigm for non-heme, metallomonooxygenases.*

EXPERIMENTAL PROCEDURES

Materials

The following materials were synthesized previously (Miller & Klinman, 1985): phenethylamine, [2,2-$^2H_2$]phenethylamine, *p*-methylphenethylamine, [2,2-$^2H_2$]-*p*-methylphenethylamine, *p*-bromophenethylamine, [2,2-$^2H_2$]*p*-bromophenethylamine, *p*-(trifluoromethyl)phenethylamine, [2,2-$^2H_2$]-*p*-(trifluoromethyl)phenethylamine. 3-Hydroxytyramine was from Calbiochem and [2,2-$^2H_2$]-3-hydroxytyramine was from MDS Isotopes. Fumarate was from Sigma and L-ascorbate was from Aldrich. All other chemicals used in this study were at least reagent grade. Preparation of dopamine β-monooxygenase was as described elsewhere (Stewart & Klinman, 1987).

Methods

Construction of a Vacuum Apparatus for O-18 Isotopic Experiments. A vacuum apparatus for the isolation of O_2 and conversion of isolated O_2 to CO_2 was constructed according to Guy et al. (1987) with modifications (Tian & Klinman, 1993). The collapsible reaction vehicle used by Guy et al. (1987) was replaced by a syringelike glass container adapted with a rubber plunger of a 60-mL disposable plastic syringe (Figure 1). A loop-type furnace with the heating wire wrapped outside of the furnace was constructed in place of a furnace with an internal heating wire (Guy et al., 1987). The loop-type furnace allows gas circulation inside of the furnace and therefore facilitates conversion of O_2 to CO_2 in the presence of N_2. The remaining parts of the apparatus were the same or very similar to those of Guy et al. (1987). All of the high-vacuum stopcocks, a bubbler, and cold trap used in the construction were from CalGlass. Brass and stainless steel iron fittings and valves were purchased from Oakland Valves and Fitting Co. Vacuum gauges and a pressure transducer were from Varian. Graphite rods were from Fischer.

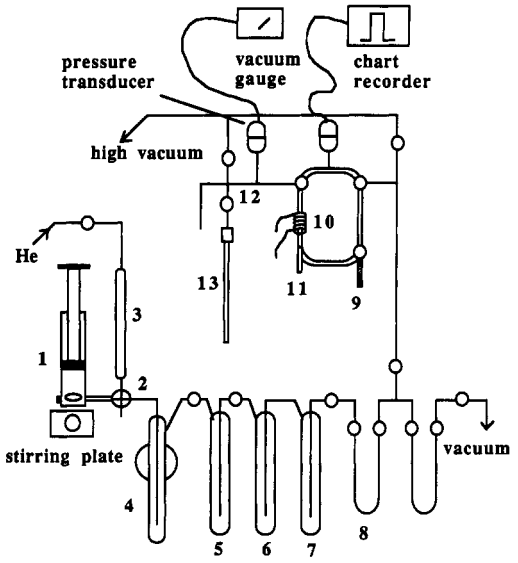

FIGURE 1: Schematic representation of the vacuum apparatus used for isolation of O_2 from reaction solutions and conversion of the isolated O_2 to CO_2.

Deuterium Isotope Effects. All of the reactions were run at 25 °C in 0.050 M phosphate buffer, pH 5.5, containing 0.100 M NaCl and 0.010 M fumarate. Reaction rates with either protonated or deuterated substrates were determined with an oxygen electrode in a reaction cell thermostated by a circulating water bath. A typical reaction mixture (2 mL) contained 10 mM ascorbate, 10 μg/mL catalase, and sufficient amount of substrate to ensure >95% saturation. The O_2 concentration was varied by blowing a mixture of O_2 and N_2 over the surface of the reaction solution while stirring. The reaction mixture was then incubated for *ca.* 5 min and the reaction initiated by addition of enzyme. Changes in O_2 concentration were followed by a YSI Model 53 biological oxygen monitor from Yellow Springs Instrument Co. The initial velocity data were fitted by a BASIC version of the HYPER program (Cleland, 1979) to

$$v = \frac{V[O_2]}{K_{O_2} + [O_2]} \quad (4)$$

where v is the initial rate, V is the maximum velocity, and K_{O_2} is the Michealis–Menten constant for O_2. Deuterium isotope effects were calculated as the ratio $(V/K_{O_2})_H/(V/K_{O_2})_D = {}^D(V/K_{O_2})$.

O-18 Isotope Effects. Conditions for determination of O-18 isotope effects were the same as for deuterium isotope effects described above. O-18 effects were measured by a competitive method involving isolation of O_2 remaining in the reaction mixture, followed by determination of the extent of reaction (f) and the isotope ratio ($R = {}^{18}O/{}^{16}O$) in the isolated oxygen. As described earlier (Tian & Klinman, 1993), all measurements are natural abundance O-18; in the event of unsymmetrical intermediates, measured values are approximated by the average of effects arising at each position. The data were fitted to eq 5 using a nonlinear least-squares routine, SYSTAT.

$$R/R_0 = (1 - f)^{[1/[{}^{18}(V/K)-1]]} \quad (5)$$

where R_0 is the isotope ratio of the blank.

Isolation of O_2 from the reaction solution and conversion of O_2 to CO_2 was initially carried out according to Guy et al. (1987) and, later, by a modified procedure described below. First, about 100–150 mL of phosphate buffer (0.05 M phosphate, 0.1 M NaCl, and 0.01 M fumarate, pH 5.5) was saturated with O_2 by blowing pure O_2 through the buffer solution in a flask for *ca.* 20 min. The O_2-saturated buffer was then pressurized into the syringelike container (**1** in Figure 1) through the four-way stopcock (**2** in Figure 1). The total volume of the container was *ca.* 70 mL. After *ca.* 35 mL of the buffer was added to the container, a preweighed solid substrate (as the amine hydrochloride) and a concentrated ascorbate solution (200 mM) were added to the buffer. After the solid was completely dissolved by stirring, the container was filled up with the buffer and the solution was well mixed by a stirring bar inside the container. Any contaminating air bubbles were carefully removed with a pipette. A rubber plunger was then inserted into the syringelike container. A sample was removed to the fixed-volume glass tube (**3**, *ca.* 16 mL) under vacuum through the four-way stopcock (**2**); the O_2 in this sample was isolated and converted to CO_2 (see below). A Dβ M solution was then injected into the reaction container through the rubber stopper of the container and mixed with the solution by the stirring bar. After a certain period of time, a sample was removed and the O_2 was isolated and converted to CO_2. The pH of the reaction mixture was routinely checked and always found to be within 5.5 ± 0.1.

Isolation of O_2 and conversion to CO_2 were carried out in a vacuum apparatus according to the following procedure. The sample taken from the reaction mixture was delivered into the bubbler (**4**) and mixed with 0.5 mL of 85% phosphoric acid which had been placed in the bubbler. O_2 was removed from the phosphate quenched solution by He sparging. The He used for sparging had been prepurified by a molecular sieve (4 Å) trap at liquid nitrogen temperature. The water vapor and carbon dioxide in the He stream from the bubbler were removed by three liquid nitrogen traps (**5**, **6**, and **7**), and O_2 and N_2 in the He stream were retained by a molecular sieve (13 Å) trap (**8**) at liquid nitrogen temperature. After 20 min, the sparging was terminated and the trapped O_2 and N_2 mixture was released by warming the trap up to 100 °C. This gas mixture was then transferred to another molecular sieve (13 Å) (**9**) and finally released to the furnace loop. Inside the latter (**10**) was a piece of graphite, wrapped with a platinum wire which serves as a catalyst for O_2 to CO_2 conversion. To convert O_2 to CO_2, the graphite was heated to about 900 °C by an external heating wire. The CO_2 formed was condensed out of the gas mixture into a glass tube (**11**) at liquid nitrogen temperature. After a 20-min conversion, the loop was evacuated, another portion of the gas mixture in the trap (**9**) was released into the furnace, and the conversion procedure was repeated. After completion of the O_2 to CO_2 conversion, the CO_2 was transferred to a pressure transducer (**12**), allowing measurement of the total CO_2 concentration. Finally, the CO_2 was trapped into a glass tube (**13**), which was sealed and sent to Krueger Enterprises in Cambridge, MA, for analysis of isotope ratio by mass ratio spectrometry. The relative pressure values of CO_2 from blank and reaction samples were used to calculate the extent of reaction, f, and the isotope ratios were used to calculate R/R_0. The resulting f and R/R_0 values were employed in least-squares analysis of eq 5.

RESULTS AND DISCUSSION

The Double Isotope Effect Does Not Allow Mechanistic Predictions in Multistep Perturbation Reactions. A particularly powerful method for the elucidation of reaction intermediates in enzymatic systems is the double isotope effect method (Hermes et al., 1982). This method involves the measurement of heavy atom isotope effects with and without

Scheme 2: General Kinetic Mechanism for DβM[a]

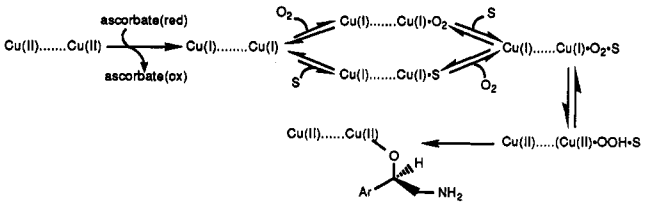

[a] The mechanism illustrates the (random) binding of O_2 and substrate to the reduced, Cu(I) form of DβM.

deuteration of substrate. The change in size of the heavy atom isotope effect as a function of substrate deuteration is used to indicate whether cleavage of bonds to hydrogen and the heavy atom occur in a stepwise or a concerted manner: in general, an increase in the size of the heavy atom isotope effect following deuteration indicates a concerted process for bond cleavage events, whereas a decrease in the heavy isotope effect is taken as evidence for a chemical intermediate. This approach has been used successfully in a number of reactions which involve one-step perturbations, in particular decarboxylation reactions [cf. a review by O'Leary (1989)].

In the present study we have begun an exploration of O-18 isotope effects in O_2-dependent enzyme reactions, in an effort to introduce a new tool for the characterization of oxygen species catalyzing C–H abstraction. An examination of the DβM reaction indicates that, in addition to the C–H cleavage step, a large number of other reversible steps are likely to be sensitive to an $^{16}O/^{18}O$ discrimination: these include the oxygen binding step, the formation of a copper hydroperoxide species (Scheme 2), and the possible intermediacy of a copper–oxo species[2] (eq 3). We have, therefore, examined whether the direction of change in an oxygen isotope effect following substrate deuteration can distinguish between a copper–hydroperoxy mechanism, eq 2, and a copper–oxo mechanism, eq 3.

It can be shown (Tian, 1992)[3] that for a linear multistep reaction where more than one step is isotope-sensitive, the O-18 isotope effect can be expressed as

$$^{18}(V/K)_H = \frac{^{18}K^{18}k + C_f' + C_r'}{1 + C_f + C_r} \quad (6)$$

where ^{18}k is the intrinsic kinetic isotope effect on the C–H cleavage step and ^{18}K is the overall equilibrium isotope effect on the steps preceding the substrate activation. C_f and C_r are the usual forward and reverse commitments (Northrop, 1977). C_f' and C_r' are composed of products of isotope effects for steps preceding the catalytic step and commitments, such that C_f' and C_r' can be either larger or smaller than C_f and C_r, depending on whether the isotope effects are normal or inverse. In the case of DβM, measurements have been collected under

Scheme 3: Alternative Mechanisms for Substrate Hydroxylation[a]

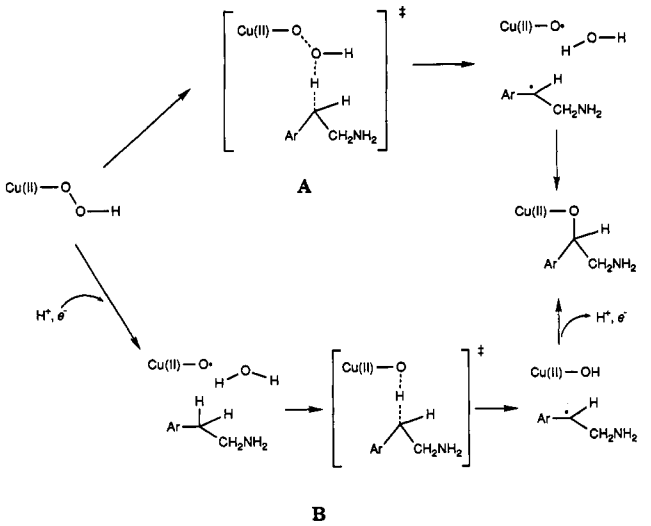

[a] Either a copper–hydroperoxo species (A) or a copper–oxo species (B) acts as the hydroxylating agent.

conditions of an ordered kinetic mechanism with substrate binding before O_2:

$$E{\cdot}S + O_2 \underset{k_2}{\overset{k_1}{\rightleftharpoons}} E{\cdot}S{\cdot}O_2 \underset{k_4}{\overset{k_3}{\rightleftharpoons}} E{\cdot}I \xrightarrow{k_5} E + P \quad (7)$$

where S is the phenethylamine substrate, I is an intermediate, and P is the product. Since the reverse commitment is zero (Miller & Klinman, 1983), eq 6 reduces to

$$^{18}(V/K)_H = \frac{^{18}K^{18}k + C_f'}{1 + C_f} \quad (8)$$

where ^{18}k is the intrinsic isotope effect on k_5 and ^{18}K is the equilibrium isotope effect on K_1K_3 ($K_1 = k_1/k_2$ and $K_3 = k_3/k_4$). Additionally, $C_f = (k_5/k_4)[1 + (k_3/k_2)]$ and $C_f' = (k_5/k_4)[^{18}K_1{}^{18}k_3 + (^{18}k_1k_3/k_2)]$. The double isotope effect for deuterated substrate can be shown to be

$$^{18}(V/K)_D = \frac{^{18}K^{18}k + C_f'/{}^Dk}{1 + C_f/{}^Dk} \quad (9)$$

where ^Dk is the intrinsic deuterium isotope effect on k_5. According to this equation, deuteration will reduce C_f and C_f', thereby increasing the expression of the intrinsic O-18 isotope effect on the C–H abstraction step, independent of mechanism. For more complex mechanisms, in which the reverse commitment is nonnegligible, it can also be shown that deuteration can only increase the expression of $^{18}K^{18}k$. We therefore conclude that for reactions in which heavy atom isotope effects appear on multiple steps, the direction of change in the O-18 isotope effects as a function of substrate deuteration cannot provide insight into the mechanism of C–H cleavage.

Magnitude of Intrinsic O-18 Isotope Effects as a Predictor of Mechanism. In light of our inability to use double isotope effects to probe the nature of oxygen intermediates in monooxygenase-catalyzed C–H abstractions, we turned to the size of the isotope effect as a probe of mechanism. From the outset it was clear that the magnitude of the intrinsic isotope effect for a single substrate could not, in general, distinguish mechanism. It is useful to consider this statement in the context of the two possible pathways proposed for DβM (Scheme 3). For the copper–oxy mechanism (Scheme 3B) the terminal oxygen of copper hydroperoxide has been

[2] Intermediates formed from oxygen are expected to be increasingly high-energy species which lie between the enzyme ternary complex and the transition state for C–H bond cleavage. In this manner, the interconversion of all such species will be reversible. Reversibility is supported by an observed dependence of O-18 isotope effects on substrate structure and deuteration (cf. Table I) as well as earlier reports of deuterium isotope effects on V_{max}/K_m (Miller & Klinman, 1985).

[3] An early treatment of isotope effects corresponding to multistep perturbations was given by Schowen (1978). A formulation considering the contribution from the intrinsic kinetic isotope effect of each step was put forth by Stein (1981), which has been applied to secondary hydrogen isotope effects in a few enzymatic reactions (Stein et al., 1984; Alvarez et al., 1991). Tian (1992) treated contributions from both the kinetic and the equilibrium isotope effects, and this procedure was used to derive the isotope effect equations in this paper.

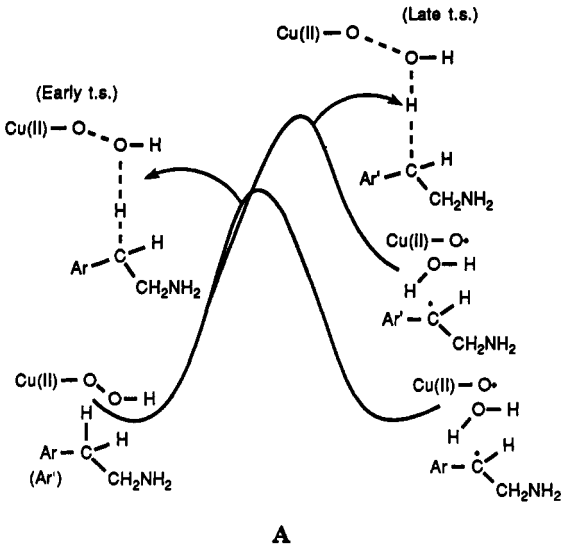

FIGURE 2: Change in transition-state structure with changes in substrate reactivity for a copper–peroxo mechanism (A) and a copper–oxo mechanism (B).

transformed to water prior to the hydrogen abstraction step, leading to a conservation of bond order at this oxygen. Similarly, for the copper–hydroperoxy mechanism (Scheme 3A), O–O bond cleavage at the transition state involving hydrogen abstraction from substrate is compensated by O–H bond formation at the terminal oxygen, leading (more or less) to a conservation of bond order at this position. Consequently, the bond order to the terminal oxygen of the initial copper–hydroperoxy species is not expected to be very sensitive to mechanism. Pathways A and B in Scheme 3 do, however, predict different bond order changes at the oxygen bonded directly to copper, with pathway B predicting an increase in bond order at the C–H cleavage step whereas pathway A predicts a decrease in bond order. In the event that the O-18 isotope effect could be measured on this single step, one would predict a normal O-18 isotope effect for the copper–peroxy mechanism and an inverse isotope effect for the copper–oxo mechanism. However, as shown by eq 8, the experimentally accessible intrinsic O-18 isotope effect is the product of isotope effects on all steps leading from unbound O_2 to the transition state involving C–H activation. Since both pathways A and B show considerable decrease in bond order at the oxygen bound to copper at the transition state, both mechanisms predict normal O-18 isotope effects.

As described by Miller and Klinman (1985), DβM displays a broad substrate specificity toward ring-substituted phenethylamines, with the rate of C–H activation increasing from 2 to 700 s^{-1} as ring substitution varies from 4-(trifluoromethyl)- to 3,4-dihydroxyphenethylamine (dopamine). Although ring substituents may also influence, to some extent, the rate of O_2 binding and its reductive activation to a peroxy or oxo species, it is highly unlikely that changes in substrate structure will alter the O-18 isotope effects for these equilibrium steps involving O_2. *With the expectation that changes in O-18 isotope effect with variations in substrate reactivity will be restricted to the C–H cleavage step, a basis for distinguishing mechanism emerges.* This is illustrated in Figure 2, panels A and B for the copper–peroxy and copper–oxo mechanisms, respectively. As shown for the copper–peroxy pathway (Figure 2A), changes in substrate structure which lead to a later transition state produce a greater loss in bond order at the oxygen bound to copper and hence the prediction of a more normal O-18 isotope effect. By contrast, the copper–oxo pathway (Figure 2B) predicts that substrates producing a later transition state will be characterized by increased bond order to oxygen and smaller O-18 isotope effects.

Table 1: Kinetic Isotope Effects for DβM[a]

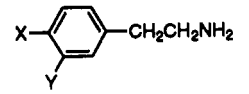

X	Y	$^{D}(V/K)$	$^{18}(V/K)_H$	$^{18}(V/K)_D$
OH	OH	3.68 ± 0.56	1.0197 ± 0.0003	1.0256 ± 0.0003
H	H	4.35 ± 0.46	1.0179 ± 0.0002	1.0238 ± 0.0006
CH_3	H	6.50 ± 0.51	1.0212 ± 0.0008	1.0232 ± 0.0009
Br	H	11.85 ± 0.62	1.0205 ± 0.0001	1.0214 ± 0.0001
CF_3	H	18.50 ± 1.40	1.0215 ± 0.0003	1.0216 ± 0.0003

[a] Data collected at pH 5.5, 25 °C, 10 mM fumarate; these conditions lead to a kinetically ordered mechanism where substrate binds first.

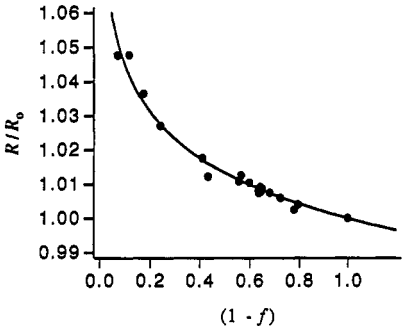

FIGURE 3: Plot of the theoretical curve of R/R_0 vs $(1-f)$ according to eq 5 using $^{18}(V/K) = 1.0281$ (for the substrate dopamine). The experimental data are shown by the closed circles.

Intrinsic O-18 Isotope Effects as a Function of Substrate Structure in the DβM Reaction. In Table 1 we summarize the results of the measurement of O-18 isotope effect for a series of ring-substituted phenethylamines using substrates which are either protonated or dideuterated at C-2. In the determination of $^{18}(V/K)_H$ or $^{18}(V/K)_D$, a minimum of 10 data points were collected and fitted to eq 5 to abstract the value of the isotope effect. Figure 3 shows a typical data set (for dopamine), where the solid line is the theoretical curve of eq 5. Deuterium isotope effects have also been measured under the same experimental conditions as O-18 effects and are included in Table 1. One feature of the data in Table 1 that has been noted previously is the large range in the magnitude of deuterium isotope effects, reflecting an increasing rate limitation of the C–H cleavage step in proceeding from electron-releasing to electron-withdrawing substituents. This effect is carried over to O-18 isotope effects, such that the

Table 2: Intrinsic O-18 Isotope Effects in the DβM Reaction

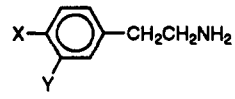

X	Y	k^a (s^{-1})	$^{18}K^{18}k^b$	$^{18}k^c$
OH	OH	680	1.0281 ± 0.0012	1.0166
H	H	500 (0.18)[d]	1.0256 ± 0.0008	1.0141
CH_3	H	140 (0.93)	1.0236 ± 0.0011	1.0122
Br	H	22 (2.03)	1.0215 ± 0.0001	1.0101
CF_3	H	2 (3.46)	1.0216 ± 0.0003	1.0102

[a] From Miller and Klinman (1985). [b] From eq 10 in text and the data in Table 1. [c] Calculated, assuming $^{18}K = 1.0113$ (Tian & Klinman, 1993). [d] Increase in activation energy relative to the parent compound, in kilocalories per mole.

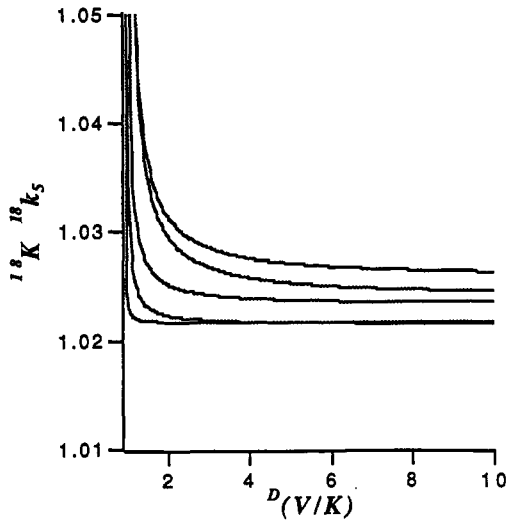

FIGURE 4: Dependence of calculated values for $^{18}K^{18}k_5$, eq 10, as a function of $^{D}(V/K)$. The curves represent the five substrates in Table 2 in order of descending reactivity.

magnitude of $^{18}(V/K)_H$ increases with electron-withdrawing substituents. It can be seen that deuteration also increases the magnitude of $^{18}(V/K)_D$ for substrates where the C–H cleavage step is only partially rate-limiting. Clearly, the measured O-18 isotope effects are complex, reflecting the contribution of multiple steps to the DβM reaction.

The intrinsic O-18 isotope effects can, however, be calculated from the available experimental data. As shown in the Appendix, use of eqs 8 and 9, together with the equation for the deuterium isotope effect, $^{D}(V/K) = (^{D}k + C_f)/(1 + C_f)$, leads to an expression for $^{18}K^{18}k$ in terms of $^{18}(V/K)_H$, $^{18}(V/K)_D$, and $^{D}(V/K)$:

$$^{18}K^{18}k = \frac{^{D}(V/K)^{18}(V/K)_D - ^{18}(V/K)_H}{^{D}(V/K) - 1} \qquad (10)$$

The values calculated for $^{18}K^{18}k$ as a function of substrate structure are summarized in Table 2, with attendant errors propagated from experimental uncertainties in $^{18}(V/K)_H$, $^{18}(V/K)_D$, and $^{D}(V/K)$. A notable feature of the data in Table 2 is the relatively small final error in $^{18}K^{18}k$. Analysis of eq 10 indicates that the uncertainty in computed values for $^{18}K^{18}k$ is highly dependent on the observed value for $^{D}(V/K)$, with values for $^{18}K^{18}k$ becoming quite reliable when $^{D}(V/K) >$ 3–4. This is illustrated graphically in Figure 4, which shows the change in computed $^{18}K^{18}k$ as a function of $^{D}(V/K)$ for each of the five substrates under investigation. Fortunately, in each case, the observed magnitude of $^{D}(V/K)$ falls in a range where $^{18}K^{18}k$ changes very little, if at all, with changes in $^{D}(V/K)$. The validity of final values for $^{18}K^{18}k$ is further supported by comparison of these values in Table 2 to those for $^{18}(V/K)_D$ in Table 1. It can be seen that deuteration of substrate reduces the magnitude of C_f and C_f' to the point where the intrinsic O-18 isotope effect is almost completely expressed and hence that mechanistic conclusions will be similar using either the experimental values for $^{18}(V/K)_D$ or the calculated values for $^{18}K^{18}k$.

As already noted, studies by Miller and Klinman (1985) provided estimates of rate constants for the C–H bond cleavage step with ring-substituted phenethylamine substrates. These rate constants have been included in Table 2, for comparison to values for $^{18}K^{18}k$. It can be seen that a trend occurs, such that the magnitude of $^{18}K^{18}k$ decreases as the rate of the reaction decreases (>300-fold); this decrease in rate correlates with a change in activation energy for C–H cleavage of ca. 3.5 kcal/mol. We have also included an estimate of values for ^{18}k using a previously measured value of ^{18}K for Fe(III)–OOH formation (Tian & Klinman, 1993) as a model for ^{18}K in Cu(II)–OOH formation from DβM and dioxygen. These estimates of ^{18}k, which are based on the assumption that ^{18}K will be independent of substrate, indicate a *ca.* 60% increase across the range of substrates studied. As we argue below, the relationship between $^{18}K^{18}k$ (or ^{18}k) and the rate of the reaction provides a unique probe of the oxygen species performing the C–H abstraction step.

Mechanistic interpretation follows from the Hammond postulate, which predicts transition-state structure from thermodynamic driving forces and rates within a series of related substrates (Hammond, 1958). According to this postulate, the position of the transition state is expected to become more productlike as the reaction driving force and rate decrease; conversely, the substrate with the largest driving force and fastest rate will be characterized by the most reactantlike transition state. Although anti-Hammond behavior can occur (*cf.* Thornton, 1967), the influence of ring substituent on the rate of the DβM-catalyzed C–H cleavage step is expected to occur primarily along the reaction coordinate (Hammond behavior). It is, therefore, possible to predict that the transition state for the fastest DβM substrate, dopamine, will be characterized by a relatively early transition state, whereas the transition state for the slowest substrate, *p*-(trifluoromethyl)phenethylamine, will occur relatively late. This interpretation is consistent with the size of deuterium isotope effects for *p*-bromo- and *p*-(trifluoromethyl) substrates, 11.9 and 18.5, respectively, both of which exceed the value of 11.2 for dopamine (Miller & Klinman, 1983). Such a trend supports the view that the transition state for C–H bond cleavage with the natural substrate dopamine is relatively early, whereas slower substrates are characterized by later, more symmetrical transition states and hence larger primary deuterium isotope effects [*cf.* Westheimer (1961) and Bell (1973)].

Initially, a mechanism in which the active oxygen species is Cu(II)–OOH has been examined (Scheme 3A). As shown in Figure 2A, early and late transition states for this mechanism differ in the amount of bond cleavage at the oxygen atom bound to copper, where the terminal O–H of the Cu(II)–OOH is assumed to experience very little change in bond order due to compensating effects of O–O bond cleavage and O–H bond making. Using the Hammond postulate to infer transition-state structure, we predict that the decrease in bond order between the O–O bond of Cu(II)–OOH should be greatest for the *p*-CF_3-phenethylamine and least for the dopamine. A corollary of this prediction is that the magnitude

of the O-18 isotope effect should increase as the rate of the reaction decreases. As seen in Table 2, this is in direct conflict with the experimental observations, leading to the conclusion that Cu(II)–OOH cannot be the species responsible for C–H activation in the DβM reaction.

Since this conclusion rests on the assumption that bond order is conserved at the terminal O–H of the Cu(II)–OOH, it is useful to consider mechanisms which are asynchronous, leading either (i) to greater O–O bond cleavage than O–H formation at the transition state or (ii) to greater O–H bond formation than O–O bond cleavage at the transition state. The latter possibility can be ruled out, since it would require that oxygen expand its octet of outer valence electrons. If O–O bond cleavage actually occurs in advance of O–H bond formation, this would only lead to a further net decrease in bond order at oxygen in the transition state and hence the prediction of an increasing O-18 isotope effect with decreasing substrate reactivity.

As an alternative to Cu(II)–OOH, a copper oxygen radical species (Cu(II)–O•) formed by reductive cleavage of the initially formed Cu(II)–OOH has been introduced (Scheme 3B). For this type of mechanism, hydrogen transfer from substrate to oxygen can only increase the bond order at oxygen. As illustrated in Figure 2B, proceeding from an early to a late transition state leads to an increase in bond order at oxygen and a concomitant decrease in the kinetic O-18 isotope effect. As a result, the mechanism shown in Scheme 3B predicts the largest isotope effect with dopamine and the smallest isotope effect with *p*-CF_3-phenethylamine, in complete accord with the experimental observations. We conclude that the observed changes in $^{18}K^{18}k$ with changes in substrate structure and rate implicate O–O cleavage prior to substrate activation, bringing the mechanism of DβM closer to models previously invoked for heme–iron systems such as cytochrome P-450 (Coon & White, 1980).

A Postulated Role for Protein Side Chains in Metal–Oxygen Activation. In light of the evidence for O–O bond cleavage prior to H abstraction from substrate in a copper-dependent monooxygenase, the question arises as to how this can be achieved. Unlike iron-dependent monooxygenases, where the metal center can exist in multiple high valence states, copper does not have ready access to valence states above +2 [for example, the redox potential for Cu(II) → Cu(III) is *ca.* 1 V (cf. Margeram et al., 1993)]. On this basis, we eliminate a mechanism involving Cu(II) to Cu(III) conversion coupled to reductive cleavage of peroxide:

$$\text{Cu(II)–OOH} \rightarrow \text{Cu(III)–O}^{\bullet} + \text{H}_2\text{O} \leftrightarrow \text{Cu(IV)–O}^{-} + \text{H}_2\text{O} \quad (11)$$

As shown in eq 11, this type of cleavage of the O–O bond produces a resonance hybrid of a Cu(III) (oxygen radical) and a Cu(IV) (oxygen anion)!

Alternatively, it is conceivable that the reactive species in DβM is Cu(I)–OOH, formed by one-electron reduction of the reaction intermediate Cu(II)–OOH. Reoxidation of Cu(I) to Cu(II) would lead to O–O bond cleavage and Cu(II)–O•:

$$\text{Cu(I)–OOH} \xrightarrow{\text{H}^+} \text{Cu(II)–O}^{\bullet} + \text{H}_2\text{O} \quad (12)$$

However, several lines of evidence argue strongly against such an external reductive cleavage mechanism. First, early observations of large deuterium isotope effects under conditions of saturating concentrations of electron donor had excluded the possibility of a compulsory binding of reductant between the steps of substrate binding and oxygen activation (Stewart & Klinman, 1987). Second, pre-steady-state kinetics of the reduced, Cu(I), form of DβM indicate it is fully catalytically competent in the absence of further electron input (Brenner & Klinman, 1989).

Recent studies from this laboratory on substrate analogs of the DβM reaction (Kim & Klinman, 1991) provide possible insight into a mechanism for Cu(II)–OOH reductive activation. As shown below, a series of compounds, **1**, **3**, and **4**, have been studied, which can be considered subsets of the substrates dopamine and tyramine: Additionally, the behavior

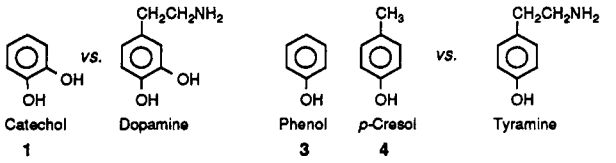

of a *p*-quinol, HO-C_6H_4-OH (**2**), has been examined for comparison to catechol (**1**). Compounds **1–4** all show inhibitor activity toward DβM. Enzyme turnover is also observed, with the exception of phenol, placing compounds **1**, **2**, and **4** in the category of mechanism-based inhibitors. Unexpectedly, the rate of enzyme inactivation with phenol was found to be comparable to *p*-cresol, despite the fact that phenol is incapable of supporting enzyme turnover.

In an effort to gain mechanistic insight into the interaction of **1–4** with DβM, a series of solvent and substrate isotope effects have been investigated (Kim & Klinman, 1991). The solvent isotope effects with quinols **1** and **2** were found to be quite small, ranging from 1.7 to 2.5 for both turnover and inactivation. Given the ease with which quinols can undergo 1-e^- oxidation processes, the origin of these small values has been attributed to a combination of (secondary) effects on the formation of radical cation, which then partitions further between a 1-e^- oxidation to yield enzyme-bound quinone and enzyme inactivation. The results of solvent isotope effect determinations with phenols **3** and **4** were found to be very different from those with quinols, revealing differential effects on turnover ($^Dk_{cat} \simeq 1$) *vs.* inactivation ($^Dk_i = 6–7$). The extremely large magnitude of ^Dk_i has led to the conclusion of a rate-limiting abstraction of hydrogen from the solvent-exchangeable, phenolic hydroxyl group in the course of enzyme inactivation.

Consistent with the expectation that enzyme turnover would involve C–H bond cleavage, isotope effects using perdeuterated *p*-cresol indicated a reversal of effects seen with solvent D_2O, such that $^Dk_{cat} = 5$ and $^Dk_i \simeq 1$ (Kim & Klinman, 1991). From such behavior it became clear that *p*-cresol was capable of dual binding modes, one of which led to turnover and the other to inactivation (Scheme 4). The small size of cresol, relative to the phenethylamine substrates, is proposed to lead to more than one orientation for *p*-cresol within the binding site. Analogous to normal amine substrates, the methyl group of cresol can bind in proximity to Cu(II)–OOH, leading to C–H activation and turnover. Alternatively, placement of the hydroxyl group of cresol near Cu(II)–OOH will produce O–H cleavage and ultimately enzyme inactivation. The slower rate of enzyme inactivation is attributed to a lower population of the reverse binding mode, since the almost identical bond dissociation energies (BDEs) for H• abstraction from a benzylic methyl group or phenolic hydroxyl group predict similar chemical reactivities.

We believe this recent evidence for a DβM-catalyzed O–H abstraction can be integrated with the demonstrated presence

Scheme 4[a]

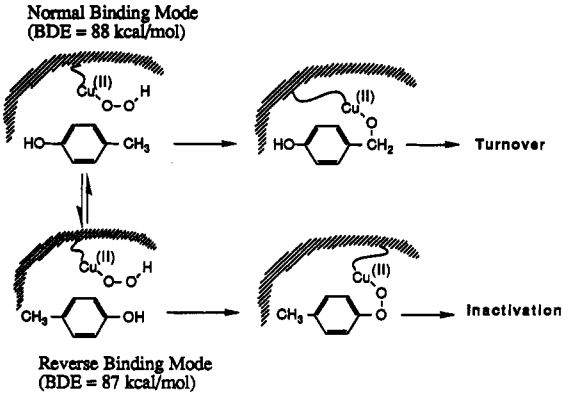

[a] As illustrated, the mechanism-based inhibitor cresol is concluded to bind to DβM in two binding modes, leading to C–H activation and enzyme turnover (A) or O–H activation and enzyme inhibition (B). From Kim and Klinman (1991).

Scheme 5: New Mechanism for DβM[a]

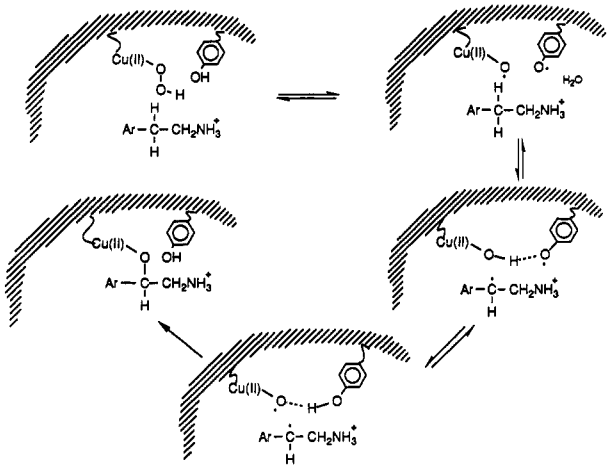

[a] This mechanism involves an obligatory cleavage of Cu(II)–OOH to generate Cu(II)–O• as the hydroxylating agent. See text for details.

of Tyr-216 and Tyr-357 at or near the enzyme active site (Fitzpatrick & Villafranca, 1987; DeWolf et al., 1988) to explain the trend in kinetic oxygen isotope effects observed in DβM catalysis (Table 2). A new reaction mechanism is introduced (Scheme 5) showing hydrogen transfer from the phenolic group of an active-site tyrosine to Cu(II)–OOH. As illustrated, this reaction generates Cu(II)–O• as the substrate hydroxylating agent. Hydrogen abstraction from the β-carbon of substrate produces a hydrogen-bonded intermediate, which equilibrates between a Cu(II)–OH/tyrosyl radical and a Cu(II)–O•/tyrosine. Rebound of the substrate-derived benzylic radical with the latter species leads to a product alkoxide liganded to copper and the regeneration of the active-site tyrosine. In light of the almost identical bond dissociation energies for H abstraction from phenolic and benzylic positions, activation of the Cu(II)–OOH via a tyrosyl O–H cleavage does not offer an energetic advantage, relative to a direct C–H abstraction from phenethylamines. We propose, instead, an evolutionary advantage to the formation of protein-derived functional units for oxygen activation [Cu(II)–OOH and tyrosine in the case of DβM], providing independent reactive species with the potential to oxidize a wide range of organic substrates. It will, therefore, be very interesting to see if the type of chemistry proposed in Scheme 5 can be generalized to other non-heme, metalloenzyme systems. In the case of DβM, our proposed mechanism can be tested by selective substitution of tyrosine residues by phenylalanines, although these experiments must await the successful expression of the cloned DβM genes (Lamouroux et al., 1987; Taljanidisz et al., 1989; Lewis et al., 1990).

In recent years, protein-centered radicals in enzymatic catalysis have received increasing attention (Prince, 1988; Stubbe, 1989). A classical example is the demonstration of a tyrosyl radical in the catalysis of *Escherichia coli* ribonucleotide reductase (Reichard & Ehrenberg, 1983). It has also been demonstrated that two tyrosyl radicals are involved in the function of chloroplast photosystem II (Styring & Rutherford, 1987; Dreyfus et al., 1988) and a single tyrosyl radical in the function of prostaglandin H synthase (Karthein et al., 1988), as well as a modified tyrosyl radical in galactose oxidase (Itoh et al., 1991). With regard to other protein side chains, a tryptophan residue has been demonstrated in cytochrome *c* peroxidase (Sivaraja et al., 1989) and a glycyl radical in pyruvate formate lyase (Wagner et al., 1992). These findings indicate that protein centered radicals in oxidoreductases may not be a rare phenomenon. With the data presented herein, we raise the possibility that non-heme, metallomonooxygenases may join the ranks of proteins which utilize amino-acid-derived radical centers in their catalytic cycle.

APPENDIX

Derivation of the Equation of $^{18}K^{18}k$, in Terms of Measured Isotope Effects. The oxygen-18 isotope effect, the double isotope effect, and the deuterium isotope effect on the DβH reaction are given by, respectively,

$$^{18}(V/K)_H = \frac{^{18}K^{18}k_5 + C_f'}{1 + C_f} \quad \text{(A1)}$$

$$^{18}(V/K)_D = \frac{^{18}K^{18}k_5 + C_f'/^Dk_5}{1 + C_f/^Dk_5} \quad \text{(A2)}$$

and

$$^D(V/K) = \frac{^Dk_5 + C_f}{1 + C_f} \quad \text{(A3)}$$

From eq A1 we have

$$C_f' = ^{18}(V/K)_H[1 + C_f] - ^{18}K^{18}k_5 \quad \text{(A4)}$$

and from eq A2 we have

$$C_f' = ^{18}(V/K)_D[^Dk_5 + C_f] - ^{18}K^{18}k_5{}^Dk_5 \quad \text{(A5)}$$

Comparing eqs A4 and A5,

$$^{18}(V/K)_H[1 + C_f] - ^{18}K^{18}k_5 = ^{18}(V/K)_D[^Dk_5 + C_f] - ^{18}K^{18}k_5{}^Dk_5 \quad \text{(A6)}$$

from which we have

$$^{18}K^{18}k_5[^Dk_5 - 1] = ^{18}(V/K)_D[^Dk_5 + C_f] - ^{18}(V/K)_H[1 + C_f] \quad \text{(A7)}$$

We notice that

$$[^Dk_5 - 1] = [^D(V/K) - 1][1 + C_f] \quad \text{(A8)}$$

and

$$[^Dk_5 + C_f] = ^D(V/K)[1 + C_f] \quad \text{(A9)}$$

Bringing eqs A8 and A9 into eq A7 and rearranging yields

the following equation:

$$^{18}K^{18}k_5 = \frac{^{D}(V/K)^{18}(V/K)_D - ^{18}(V/K)_H}{^{D}(V/K) - 1} \quad \text{(A10)}$$

REFERENCES

Ahn, N. G., & Klinman, J. P. (1983) *Biochemistry 22*, 3096–3106.

Alvarez, F. J., Ermer, J., Hubner, G., Schellenberger, A., & Schowen, R. L. (1991) *J. Am. Chem. Soc. 113*, 8402–8409.

Bell, R. P. (1973) *The Proton in Chemistry*, 2nd ed., Cornell University Press, Ithaca, NY.

Blackburn, N. J., Pettingill, T. M., Seagraves, K. S., & Shigeta, R. T. (1990) *J. Biol. Chem. 265*, 15383–15386.

Brenner, M., & Klinman, J. P. (1988) *Biochemistry 28*, 4664–4670.

Cleland, W. W. (1979) *Methods Enzymol. 63*, 103–138.

Coon, M. J. & White, R. E. (1980) in *Metal Ion Activation of Dioxygen* (Spiro, T. G., Ed.) Chapter 2, pp 73–123, Wiley, New York.

DeWolf, W. E., Jr., Carr, S. A., Varrichio, A., Goodhart, P. J., Mentzer, M. A., Roberts, G. D., Southan, C., Dolle, R. E., & Kruse, L. I. (1988) *Biochemistry 27*, 9093–9101.

Dreyfus, R. J., Barry, B. A., Babcock, G. T., & McIntosh, L. (1988) *Proc. Natl. Acad. Sci. U.S.A. 85*, 427–430.

Fitzpatrick, P. F., & Villafranca, J. J. (1987) *Arch. Biochem. Biophys. 257*, 231–238.

Fitzpatrick, P. F., Flory, D. R., Jr., & Villafranca, J. J. (1985) *Biochemistry 24*, 2108–2114.

Guy, R. D., Fogel, M. F., Berry, J. A., & Hoering, T. C. (1987) *Prog. Photosynth. Res. 3*, 597–600.

Hammond, G. S. (1955) *J. Am. Chem. Soc. 77*, 334–338.

Hermes, J. D., Roeske, C. A., O'Leary, M. H., & Cleland, W. W. (1982) *Biochemistry 21*, 5106–5114.

Itoh, N., Phillips, S. E. V., Stevens, C., Ogel, Z. B., McPherson, M. J., Keen, J. N., Yadav, K. D. S., & Knowles, P. F. (1991) *Nature 350*, 87–90.

Karthein, R., Dietz, R., Nastainczyk, W., & Ruf, H. H. (1988) *Eur. J. Biochem. 171*, 313–320.

Kim, S.-C., & Klinman, J. P. (1991) *Biochemistry 30*, 8138–8144.

Lamouroux, I. A., Vigny, A., Biguet, N. F., Darmon, M. C., Franck, R., Henry, J. P., & Mallet, J. (1987) *EMBO J. 13*, 3931–3937.

Lewis, E. J., Allison, S., Fader, D., Claflen, V., & Baizer, L. (1990) *J. Biol. Chem. 265*, 1021–1028.

Margerum, D. W., Scheper, N. M., McDonald, M. R., Fredericks, F. C., Wang, L., & Lee, H. D. (1993) in *Bioinorganic Chemistry of Copper* (Karlin, K. D., & Tyeklar, Z., Eds.) pp 213–221, Chapman and Hall, London.

McCracken, J., Desai, P. R., Papadoupoulos, N. J., Villafranca, J. J., & Peisach, J. (1988) *Biochemistry 27*, 4133–4137.

Miller, S. M., & Klinman, J. P. (1983) *Biochemistry 22*, 3091–3096.

Miller, S. M., & Klinman, J. P. (1985) *Biochemistry 24*, 2114–2127.

Northrop, D. B. (1977) in *Isotope Effects on Enzyme Catalyzed Reactions*, (Cleland, W. W., O'Leary, M. H., & Northrop, D. B., Eds.) pp 122–157, University Park Press, Baltimore, MD.

O'Leary, M. H. (1989) *Annu. Rev. Biochem. 58*, 377–401.

Prince, R. C. (1988) *Trends Biochem. Sci. 13*, 286–288.

Reichard, P., & Ehrenberg, A. (1983) *Science 221*, 514–419.

Schowen, R. L. (1978) in *Transition States of Biochemical Processes* (Gandour, R. D., & Schowen, R. L., Eds.) pp 77–114, Pienum Publishing Co.

Scott, R. A., Sullivan, R. J., DeWolf, W. E., Jr., Dolle, R. E., & Kruse, L. I. (1988) *Biochemistry 27*, 5411–5417.

Sivaraja, M., Goodin, D. B., Smith, M., & Hoffman, B. M. (1989) *Science 245*, 738–740.

Solomon, E. I., Hemming, B. L., & Root, D. E. (1993) in *Bioinorganic Chemistry of Copper* (Karlin, K. D., & Tyeklar, Z., Eds.) pp 3–20, Chapman and Hall, London.

Stein, R. L. (1981) *J. Org. Chem. 46*, 3328–3330.

Stein, R. L., Fujihara, H., Quinn, D. M., Fisher, G., Kullertz, G., Barth, A., & Schowen, R. L. (1984) *J. Am. Chem. Soc. 106*, 1457–1461.

Stewart, L. C., & Klinman, J. P. (1987) *Biochemistry 26*, 5302–5309.

Stewart, L. C., & Klinman, J. P. (1988) *Annu. Rev. Biochem. 57*, 551–592.

Stubbe, J. (1989) *Annu Rev. Biochem. 58*, 257–285.

Styring, S., & Rutherford, A. W. (1987) *Biochemistry 26*, 2401–2405.

Taljanidisz, J., Stewart, L. C., Smith, A. J., & Klinman, J. P. (1989) *Biochemistry 28*, 10054–10061.

Terland, O., & Flatmark, T. (1975) *FEBS Lett. 59*, 52–56.

Thornton,, E. R. (1967) *J. Am. Chem. Soc. 89*, 2915–2927.

Tian, G. (1992) *Bioorg. Chem. 20*, 95–106.

Tian, G., & Klinman, J. P. (1993) *J. Am. Chem. Soc.* (in press).

Wagner, A. F. V., Frey, M., Neugebauer, F. A., Schäfer, W., & Knappe, J. (1992) *Proc. Natl. Acad. Sci. U.S.A. 89*, 996–1000.

Westheimer, F. H. (1961) *Chem. Rev. 61*, 265–273.